

Theory and Simulation of EPR Orthorhombic Jahn-Teller Spectra of Cu^{2+} in $\text{Cd}_2(\text{NH}_4)_2(\text{SO}_4)_3$ Single Crystals at Different Temperatures

J B Yerima¹, A B Dikko¹ and D K De²

^{*1} Department of Physics, Modibbo Adama University of Technology Yola, Nigeria

² Department of Physics, Kaduna State University, Kaduna State, Nigeria

ABSTRACT

This paper presents the theory and simulation of the derivative line shape function of the EPR orthorhombic Jahn-Teller spectra of Cu^{2+} in $\text{Cd}_2(\text{NH}_4)_2(\text{SO}_4)_3$ single crystals. Computer simulation of the Cu^{2+} EPR spectra using the spectrum fitting technique has been carried out in the temperature range of 15-180 K. The results show excellent fit between the simulated and observed spectra. The insufficient resolution of the spectra at 15 K is attributed to the coupling of copper isotopes and its orthorhombicity to phonon-induced reorientation rate or quantum tunnelling of Cu^{2+} ions among the three JT potential wells. The splitting processes in the $3d^9$ orbital states of Cu^{2+} has been explained and in conjunction with the demands of the criterion of pure static JT systems, the random strain splitting is found to be 0.0176 cm^{-1} and 0.0342 cm^{-1} at 15 K and 180 K respectively.

Keywords: Simulation, EPR orthorhombic Jahn-Teller spectra, temperature

Date of Submission: 25 June 2014



Date of Publication: 20 July 2014

I. INTRODUCTION

Jona and Pepinsky (1956) discovered the Langbeinite family of compounds with general chemical formula $(\text{X}^+)_2(\text{Y}^{2+})_2(\text{SO}_4)_3$ where X^+ is ammonia or monovalent metal and Y^{2+} is a divalent metal. According to Babu et al (1984), many authors have carried out a number of investigations on the microscopic properties of the langbeinite family of crystals. The compound cadmium ammonium sulphate, $\text{Cd}_2(\text{NH}_4)_2(\text{SO}_4)_3$ abbreviated as CAS is isomorphous to potassium magnesium sulphate, $\text{K}_2\text{Mg}_2(\text{SO}_4)_3$ abbreviated as PMS and both are members of the langbeinite family of crystals. The detailed x-ray data regarding the atomic positions in CAS does not seem to be available in the literature but that of PMS have been reported by Zemann and Zemann (Babu *et al*, 1984). Also they stated that some authors have shown that the langbeinite family of compounds in cubic space group $\text{P}_{2/3}$ with $a=10.35 \text{ \AA}$ have four molecules per unit cell. The structure consists of a group of $(\text{SO}_4)^{2-}$ tetrahedral and Cd^{2+} metal ions. There are two each crystallographically non-equivalent Cd^{2+} and $(\text{NH}_4)^+$ sites. Each Cd^{2+} is surrounded by six oxygen atoms which form a slightly distorted octahedron. Yerima (2005, 2007) stated that EPR studies of Misra and Korezak in 1986 using Mn^{2+} as a probe revealed a phase transition at 94.5 K whose mechanism was attributed to the freezing out of the rotation of the $(\text{SO}_4)^{2-}$ ion. Also he stated that EPR studies of Mouli and Sastry in 1962 using Cu^{2+} probe at room temperature and 77 K yielded eight poorly resolved hyperfine lines in a general direction and a set of four unresolved hyperfine lines in any crystallographic plane. Their computed values of the g-factor showed that $g_{//} > g_{\perp}$ and that the A_{max} is falling along g_{min} . They concluded that Cu^{2+} ions in this system may be in a compressed octahedral position or entered into the system interstitially rather than substitutionally. The shortcomings of the study of Mouli and Sastry include its limitation to 77 K and its failure to focus on JT effect that could be associated with Cu^{2+} in this crystal as earlier hinted by Babu et al in 1984. Raman spectroscopy performed by Rabkin *et al* (1981) provided substantial information on the structural phase transition in this crystal. They observed that CAS exhibits a structural phase transition on lowering the temperature from space group $\text{p}_{2/3}$ to p_{21} at about 95 K, the lower the temperature phase being ferroelectric. Babu et al (1984) in their summary stated that Bhat *et al* (1973) EPR spectra of Mn^{2+} in the two phase groups of CAS observed at room temperature and at liquid nitrogen were slightly different, particularly in the magnitudes of their zero-field splitting, as a result of small orthorhombic component in the low temperature phase. The differences in the spectra indicated a phase transition from high temperature phase $\text{p}_{2/3}$ to a low temperature phase p_{21} . In another outlook, Yerima (2005) stated that Ng and Calvo in 1975 observed in their EPR studies using Mn^{2+} in the temperature range 300-77 K observed definite change in the spectral pattern from that of room temperature to that of liquid nitrogen temperature due to a phase transition from $\text{p}_{2/3}$ to a space group of lower symmetry at low temperature. They did not analyze the spectra nor determine the phase transition temperature due to the complexity of the spectra at liquid nitrogen temperature.

The study of phase transition in CAS using VO²⁺ as a probe in the temperature range of 573-77 K showed a complex spectrum, in which Babu et al (1984) were unable to identify the phase transition temperature and they suggested that the lower temperature phase stabilizes at temperatures higher than 95 K. This was due to a local stabilization of the low symmetry phase by vandyl ions. They also found that the data of their experiment contained Cu²⁺ ion as contaminant and thus concluded that the complication in their results could have been due to a possible JT effect associated with Cu²⁺ ion in this crystal. Unfortunately, they did not carry out further investigation to establish or rule out the possibility of JT effect due to Cu²⁺ ion in this system.

De (2010) said in order to ascertain JT effect of Cu²⁺ in CAS Oguama carried out detailed EPR study of Cu²⁺ doped in CAS at various temperatures in the range of 300-15 K with angular variations usually at steps of 5° and 0.5° near JT extrema points in three mutually perpendicular planes of CAS single crystals. The Cu²⁺:CAS spectra consists of finely resolved hyperfine lines in the low magnetic field region at all temperatures except 15 K while those in the high magnetic field region are poorly resolved at high temperatures. The complex or insufficient resolved splitting patterns of the spectra constitute a major problem in the extraction of the relevant spectroscopic parameters (resonance frequency, coupling constants, linewidths) from the spectra as starting points in the computer simulation of the spectra. Therefore, a straightforward analysis is not possible in general (neither for the human expert nor for a conceivable computer expert system (kirste, 1992)). It is against this background, several methods (spectrum contraction or elimination hyperfine splitting constants, extraction of hyperfine splitting constants, correlation method, maximum method, significance plots and ‘roll-up’ transformation) have been employed in the analysis of high resolution EPR spectra (Kirste, 1992; Wu, 2006). These methods may be more or less useful in providing estimates for the hyperfine coupling constants. On the other hand, the set of relevant spectroscopic parameters extracted from the spectra can be verified by spectrum simulation and comparison with the experimental spectrum which is the method adapted in this paper. We have adapted the spectrum fitting because it is considered an indispensable component in any scheme automated spectrum analysis.

Theory and Method of Computer Simulation of the Line Shape Function of Cu²⁺ in CAS

The detailed procedure of the experiment for determining Cu²⁺ spectra in CAS is available in Oguama (1997) and De (2010). The Oguama (1997) spectra of Cu²⁺ in this system at various temperatures were acquired for the computer simulation. The expression for the line shape function required for the computer simulation of the EPR spectra is derived from the spin Hamiltonian as follows: Thus, if the magnetic field is oriented along z-direction (100) of one of the orthorhombic JT distortions of the Cu²⁺ in CAS, the field H_z sees the g_z as well as g_x, g_y tensor axes simultaneously unlike non-JT ions, and the spin Hamiltonian H_s becomes for H along z, i.e. H_x=H_y=0.

$$H_s = \beta(H_z S_z g_z + H_x S_x g_x + H_y S_y g_y) + A_z(S_z I_z + S_x I_x + S_y I_y) + A_x(2S_x I_x + S_z I_z) + A_y(2S_y I_y + S_z I_z) \tag{1}$$

The expectation values of the Zeeman interaction for Cu²⁺ can be deduced taking into consideration the tunnel splitting equations of d⁹ ions given by (Boatner and Reynolds, 1977)

$$\begin{aligned} H_{11} &= \Gamma + \beta g_{1z} g_z S_z + A_1 S_z I_z \\ H_{22} &= \Gamma + \beta g_{2z} g_z S_z + A_2 S_z I_z \\ H_{33} &= \Gamma + \beta g_{3z} g_z S_z + A_3 S_z I_z \end{aligned} \tag{2}$$

where the terms with subscripts x or y in equation (1) vanishes i.e. H_x=H_y=0, etc. The effective Hamiltonian for Cu²⁺ is obtained by adding equations (2) bearing in mind the orthorhombic g and A tensors leading to

$$\begin{aligned} H_s &= 3\Gamma + \beta(H_z S_z g_z + H_x S_x g_x + H_y S_y g_y) + A_z(S_z I_z + S_x I_x + S_y I_y) \\ &+ A_x(2S_x I_x + S_z I_z) + A_y(2S_y I_y + S_z I_z) \end{aligned} \tag{3}$$

where 3Γ is the tunnel splitting. The knowledge of the ratio of the random strain splitting, δ̄, to the tunnel splitting, 3Γ, tells us the type of JT effect present in the system in question.

Considering the hyperfine interactions as perturbations up to second-order instead of a single transition between the non-JT Kramer’s doublet, we have three transitions for magnetic field parallel z direction (in the case of a single Cu²⁺ per unit cell in the static JT regime) for JT Kramer’s doublet as follows (assuming that the principal axis of the g-tensor ellipsoid coincides, in orientation, with the principal axes of the hyperfine terms):

$$h\nu = \beta g_z H_{zz} + A_z M_I + \frac{(A_x^2 + A_y^2)}{4\beta g_z H_{zz}} (I(I+1) - M_I^2) \quad 4$$

$$h\nu = \beta g_x H_{xx} + A_x M_I + \frac{(A_z^2)}{2\beta g_x H_{xx}} (I(I+1) - M_I^2) \quad 5$$

$$h\nu = \beta g_y H_{yy} + A_y M_I + \frac{(A_z^2)}{2\beta g_y H_{yy}} (I(I+1) - M_I^2) \quad 6$$

Now considering only the first order terms in equations 4-6 the function describing line shapes in a non-JT complex for H along any g direction may be given by $V(H) = H - \frac{h\nu}{\beta g} + AM_I$. Thus, following the theory of the orthorhombic JT complex and considering transitions in equations 4-6, the resultant line shape function will be simultaneously governed by three functions given by

$$V_1(H) = H - \frac{h\nu}{\beta g_z} + A_z M_I \quad 7$$

$$V_2(H) = H - \frac{h\nu}{\beta g_x} + A_x M_I \quad 8$$

$$V_3(H) = H - \frac{h\nu}{\beta g_y} + A_y M_I \quad 9$$

Thus the expression for the derivative EPR line shape can be written as

$$F'(H) = -2k \int_0^{\pi/2} \left[\frac{P_1(\phi)V_1}{(V_1^2 + R_1)^2} + \frac{P_2(\phi)V_2}{(V_2^2 + R_2)^2} + \frac{P_3(\phi)V_3}{(V_3^2 + R_3)^2} \right] d\phi \quad 10$$

where $P_1 = g_z^2(g_x^4 - g_y^4)\cos^2\phi + g_y^4 + \frac{g_z^2 g_y^2}{\delta_1^2}$, $P_2 = g_x^2(g_z^4 - g_y^4)\cos^2\phi + g_y^4 + \frac{g_z^2 g_y^2}{\delta_2^2}$, $P_3 = g_y^2(g_x^4 - g_z^4)\cos^2\phi + g_z^4 + \frac{g_z^2 g_x^2}{\delta_3^2}$, $R_1 = \frac{3}{4}\omega_{T_1}^2$, $R_2 = \frac{3}{4}\omega_{T_2}^2$, $R_3 = \frac{3}{4}\omega_{T_3}^2$, $\delta^2 = g_x^2 \cos^2\phi + g_y^2(1 - x^2)$, $x = \cos\theta = 1$, $\delta_1 = g_x \cos\phi$, $\delta_2 = g_y \cos\phi$, $\delta_3 = g_z \cos\phi$

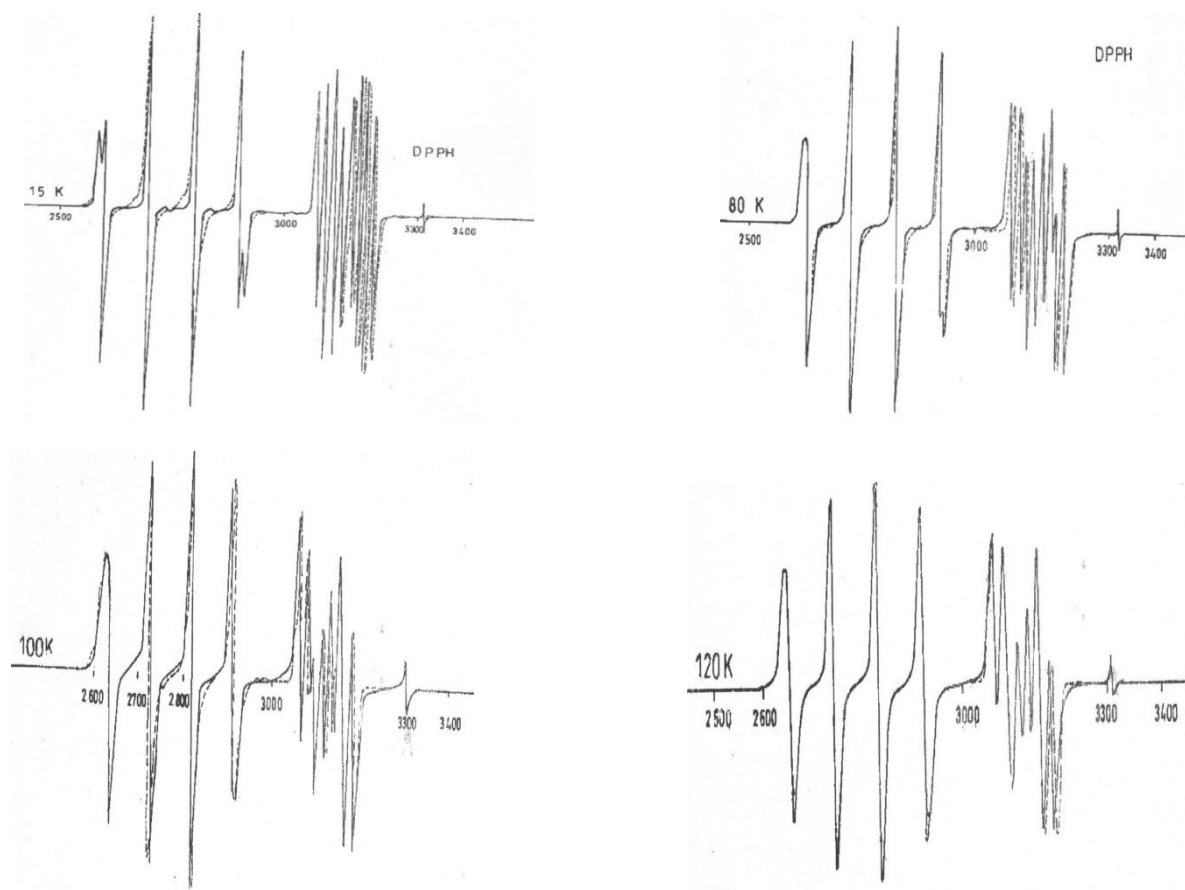
with $\omega_{T(1,2,3)}$ being the peak-to-peak linewidth (ΔH_{pp}). Finally integrating equation (10), the derivative line shape function of EPR spectra of Cu^{2+} manifesting static JT effect with orthorhombic g and A tensors in CAS is given by

$$F'(H) = -\{2\alpha f_1\} \left[\frac{H - \frac{h\nu}{\beta g_z} + A_z M_I}{\left(\left(H - \frac{h\nu}{\beta g_z} + A_z M_I \right)^2 + R_1 \right)^2} \right] - \{2\alpha f_2\} \left[\frac{H - \frac{h\nu}{\beta g_x} + A_x M_I}{\left(\left(H - \frac{h\nu}{\beta g_x} + A_x M_I \right)^2 + R_2 \right)^2} \right] - \{2\alpha f_3\} \left[\frac{H - \frac{h\nu}{\beta g_y} + A_y M_I}{\left(\left(H - \frac{h\nu}{\beta g_y} + A_y M_I \right)^2 + R_3 \right)^2} \right] \quad 11$$

where $f_1 = g_z^2(g_x^4 - g_y^2)\frac{\pi}{2} + \pi g_y^4$, $f_2 = g_x^2(g_z^4 - g_y^2)\frac{\pi}{2} + \pi g_y^4$, $f_3 = g_y^2(g_x^4 - g_z^2)\frac{\pi}{2} + \pi g_z^4$, α is the fractional relative abundance of copper isotopes $\alpha(\text{Cu}^{63}) = 0.69$ and $\alpha(\text{Cu}^{65}) = 0.31$; g_x, g_y, g_z are g-factors along the x-, y-, and z-axes respectively; H is the applied magnetic field; A_x, A_y, A_z are the hyperfine constants in the x-, y-, and z-axes respectively; R_1, R_2, R_3 are the linewidth parameters in the x-, y-, and z-axes respectively; $M_I = -3/2, -1/2, 1/2, 3/2$ and β is the Bohr magneton. The terms in the curly brackets represent the magnification factor of the line shape while the terms in square brackets determine the shape of the EPR line. The spectra of Cu^{2+} in CAS at low temperatures consists of three sets of four resolved hyperfine lines in both the $g_{//}$ and g_{\perp} directions. This implies that at the point of inflection the derivative line shape function is zero or cuts the H-axis four times in each of the three sets of four resolved lines. Thus the values of H corresponding to the points of inflection or zero F(H) can be determined. This means that the terms in square brackets must be zero i.e. $H - \frac{h\nu}{\beta g} + AM = 0$. Using two values of H(H_1 and H_2) and $M_I(M_{I_1}$ and $M_{I_2})$ corresponding to inflection points where F(H)=0, the corresponding expression for hyperfine constants is given by $A_{i(i=1,2,3)} = \frac{H_2 - H_1}{M_{I_2} - M_{I_1}} = \frac{H_2 - H_1}{n-1}$ where n is the number of complete resolved hyperfine lines and n-1 gives the number of hyperfine constants. For example, for $\text{Cu}^{63} M_{I_1} = -3/2$ and $M_{I_2} = 3/2$ so that $n - 1 = M_{I_2} - M_{I_1} = 3$ which is equivalent to n = 4.

On the other hand, generally the g values are obtained by noting the middle field point H_{mf} of the hyperfine lines corresponding to $M_{I_1} = -1/2$ and $M_{I_2} = 1/2$ and using the relation $g_{i(i=x,y,z)} = \frac{h\nu}{\beta H_{mf}}$. The calculated A and g values and estimated value of peak-to-peak linewidths $\Delta H_{pp_i(i=x,y,z)}$ were used as starting points in the computer simulation process. These values of g , A and ΔH_{pp} were substituted in the expression of $F(H)$ and the resulting line shape was compared or matched with observed EPR line. The values of g , A and ΔH_{pp} were varied by small amounts in the ranges $\pm 0.005-0.01$, $\pm 0.5-1$ G, and $\pm 5-10$ G respectively around the initial values until the line that best fits the observed EPR line was obtained. The presence of M-shape at the first crest and W-shape at the last trough corresponding to $g_{//}$ lines are assumed to be due to coupling between Cu^{63} and Cu^{65} isotopes at low temperatures (Yerima, 2007). Now, if Cu^{63} was the only one present in the sample of CAS we would expect only one set of four finely resolved hyperfine $g_{//}$ lines corresponding to $M_I = -3/2, -1/2, 1/2, 3/2$ as opposed to six lines for only Cu^{65} ($M_I = -5/2, -3/2, -1/2, 1/2, 3/2, 5/2$) present. If the two copper isotopes coexist, they couple with one another giving rise to poor resolution in the form of M-shape and W-shapes as observed at the beginning and end of the $g_{//}$ lines. In this case, the isotope effect is taken into account in search for the best line of fit using computer simulation. The effective values of g , A and ΔH_{pp} corresponding to the simulated EPR lines of Cu^{2+} in CAS at different temperatures were recorded. However, the effect of isotope is neglected by setting $\alpha=1$ where there are no M- and W-shapes present in the EPR spectra.

Results and discussion



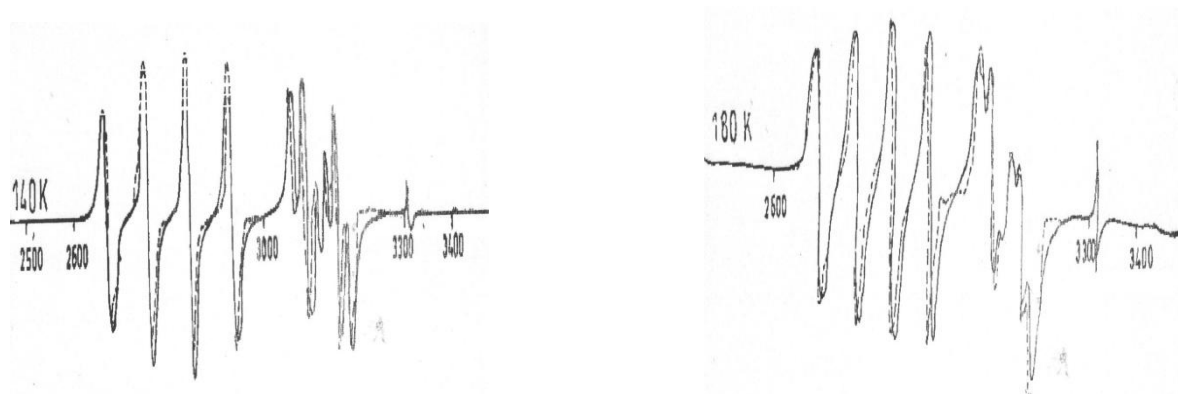


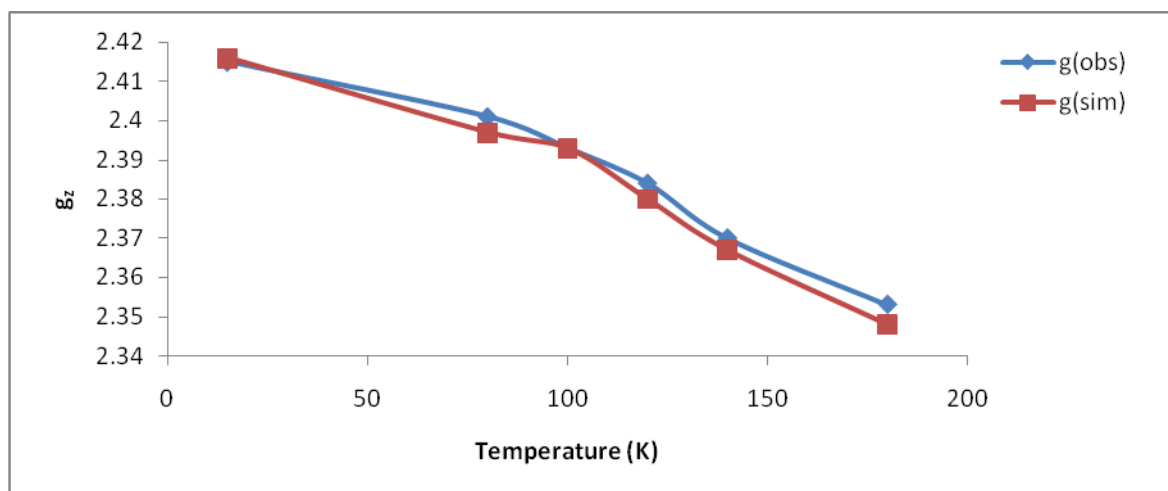
Fig. 1 Observed (solid lines) and simulated (dashed lines) spectra of Cu²⁺:CAS at different temperatures

The EPR spectra of Cu²⁺ in CAS (Fig. 1), in an ac plane, show three groups of four resolved hyperfine lines in such a way that one set appeared at the low magnetic field and the remaining two at high magnetic field. The high resolution of the spectra in the high magnetic field region at 15 K results to reduction in broadening due to spin lattice relaxation time. The solid lines represent the observed spectra while the dashed lines are the simulated spectra. The complete anisotropic spectra of the hyperfine lines in the temperature range (15 ≤ T ≤ 180 K) has been attributed to phonon-induced reorientation rate or quantum tunnelling of the Cu²⁺ ions among the three JT

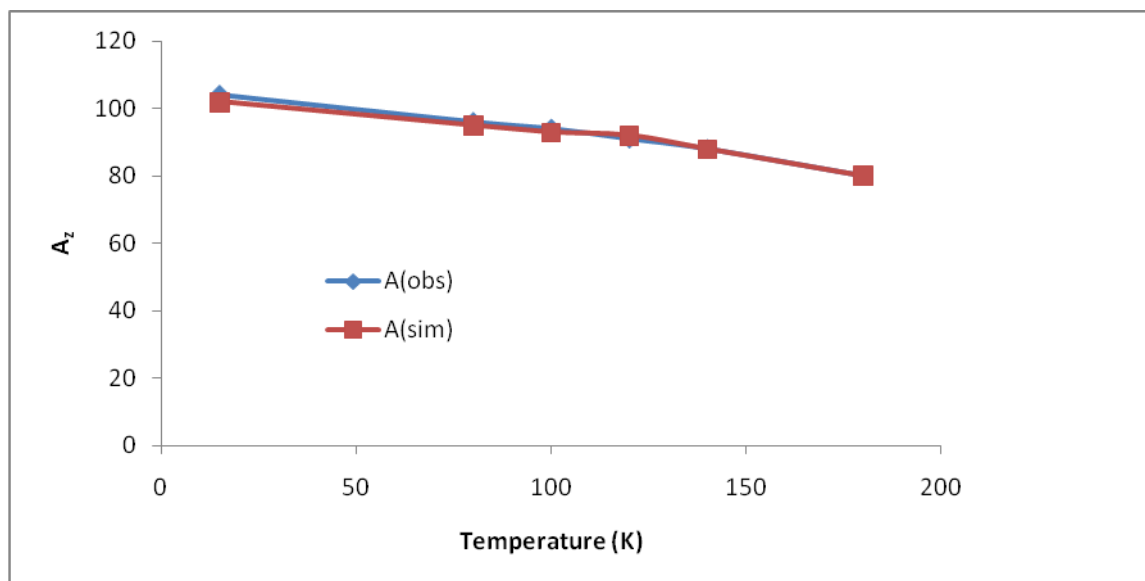
Table 1 Observed and simulated g, A and ΔH_{pp} values

T (K)	g _z	g _x	g _y	g<111>	A _z (G)	A _x (G)	A _y (G)	A<111> (G)	ΔH _{pp} (G)
15	2.415 2.416	2.144 2.136	2.094 2.093	2.222 2.214	104 102	20 20	17 16	62 62	12.0 12.0
80	2.401 2.397	2.150 2.148	2.101 2.101	2.221 2.220	96 95	12 **	* **	56 **	12.0 12.0
100	2.393 2.393	2.151 2.149	2.103 2.105	2.219 2.219	94 93	* **	* **	* **	14.0 14.2
120	2.384 2.380	* **	* **	* **	91 92	* **	* **	* **	16.0 16.3
140	2.370 2.367	* **	* **	* **	88 88	* **	* **	* **	20.0 19.8
180	2.353 2.348	* **	* **	* **	80 80	* **	* **	* **	24.0 24.8

where **bold face values** represent simulated values, * and ** represent missing observed and simulated values respectively.



(a)



(b)

Fig. 2 Variation of observed and simulated (a) g-values and (b) A-values with temperature potential wells and Cu^{2+} ions would then stabilize statistically among the three JT wells (Yerima and De, 2014). The observed and simulated values of the hyperfine coupling constant (A), g-factor (g) and peak-to-peak linewidth (ΔH_{pp}) at various temperatures are recorded in Table 1. The results show that A_z and g_z measured in the parallel direction of the magnetic field decrease with temperature while g_{\perp} (g_x, g_y) and A_{\perp} (A_x, A_y) increase with temperature.

The main difficulty in computer assisted structure elucidation consists in the extraction of the relevant spectroscopic parameters such as resonance frequency, coupling constants and linewidths from the spectra. In this study, this problem has not been solved in totality because of highly complex or insufficiently resolved splitting of the g_{\perp} lines of Cu^{2+} :CAS EPR spectra at high temperatures. However, the complete resolution of the hyperfine lines has provided reliable information that the number of equivalent nuclei in this system is three resulting to the four hyperfine lines of intensity ratios 1:3:3:1 in each of the three groups of four hyperfine lines.

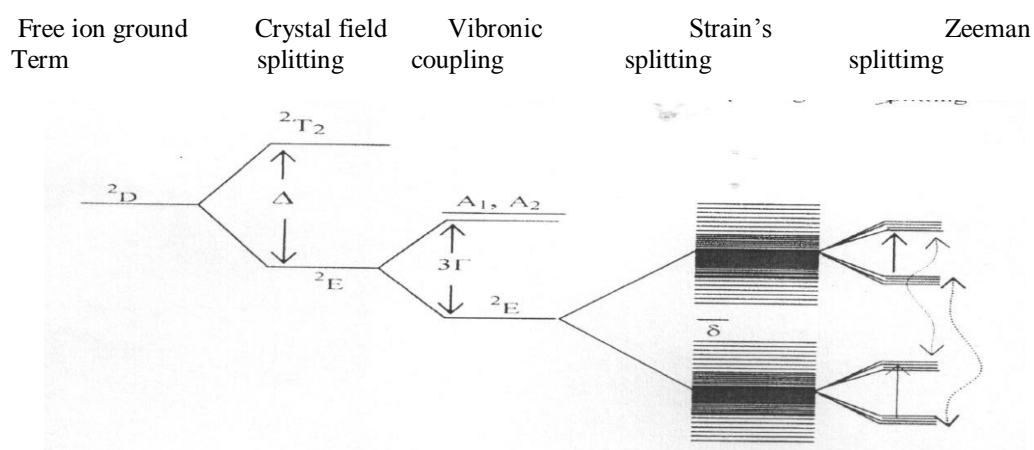

 Fig. 3 Various splitting processes of 2D ground state of Cu^{2+}

Fig. 3 shows the representation of the effects of the cubic crystal field, vibronic coupling, strain splitting, and Zeeman interaction on a 2D electronic state. Allowed $\Delta M_s = \pm 1$, $\Delta M_l = 0$ EPR transitions are indicated by straight arrows at the right hand side of the Figure. Curved arrows correspond to vibronic relaxation effects which can produce an isotropic spectrum by averaging a portion of the strained-broadened resonance pattern. A host of authors (Reynolds and Boatner, 1975; Boatner and Reynolds, 1977) have shown that for pure static JT systems like Cu^{2+} :CAS, the ratio of the random strain splitting (δ) to the tunnel splitting (3Γ) is greater than 5 i.e. $\delta \geq 5 \times 3\Gamma$. Thus, for the residual linewidth, $\Delta H_{pp} = 12$ G and $g = 2.415$ at 15 K,

$\bar{\delta} \geq 5 \times 3\Gamma = 5 \times \frac{15\sqrt{3}}{2} \Delta H_{pp} = 155.88 \text{ G} = 0.0176 \text{ cm}^{-1}$ and similarly at 180 K, $\Delta H_{pp}=24 \text{ G}$ and $g=2.353$, we have $\bar{\delta} = 0.0342 \text{ cm}^{-1}$. Thus $\bar{\delta}$ increases with temperature and is far less than the average crystal splitting $\Delta=289.6 \text{ cm}^{-1}$ (Yerima and De, 2014) computed from intensity and linewidth measurements. In the case of Cu^{2+} :CAS, the presence of M- and W-shapes at the beginning and end of the $g_{//}$ lines at low temperatures is attributed to the coupling of copper isotopes (copper 63(69%) and 65(31%)) (Yerima, 2007). The copper 63 ion has 3 equivalent protons while copper 65 ion has 4 which are expected to give 4 and 5 respectively resolved g_{\perp} or $g_{//}$ lines. At low temperatures, say 15 K, coupling of copper 65 ions becomes significant interacting with that of copper 63 ions giving rise to the M- and W-shapes. At high temperatures, copper 63 ions dominates giving rise to the four resolved $g_{//}$ lines and the g_{\perp} lines are insufficiently resolved (Fig. 1).

CONCLUSION

In this paper, the theoretical expression for the line shape function of the orthorhombic JT spectra of Cu^{2+} in CAS system have been reported. The spectra of Cu^{2+} :CAS were simulated by the aid of computer using spectrum fitting technique at various temperatures. The results show that the simulated spectra match excellently well with the observed spectra especially at the low field region where the hyperfine lines are sufficiently resolved. The splitting processes in the $3d^9$ orbital states of Cu^{2+} have been discussed. The criterion of pure static JT systems demands that the condition $\frac{\bar{\delta}}{3\Gamma} \geq 5$ must be satisfied, where $\Gamma = \frac{3\sqrt{3} H_{pp}}{2}$ and $\bar{\delta} = \frac{15\sqrt{3} H_{pp}}{2}$ the random strain splitting was found to be about 0.0176 cm^{-1} at 15 K and 0.0342 cm^{-1} at 180 K. The insufficient resolution of the spectra especially at the high magnetic field side and temperatures is attributed to the rate of coupling of copper ions in this system.

REFERENCES

- [1]. Babu D. S, Sastry G. S, Sastry M. D and Dalvi A. G. I (1984) Structural phase transition in Langbeinites an EPR study, *J. Phys. C. Solid state Phys.* 17, 4245
- [2]. Boatner L. A, Reynolds R. W, Chen Y and Abraham M. M (1977) Static, quasistatic and quasidynamic Jahn Teller effect in EPR spectra of Ag^+SrO , CaO and MgO . *Phys. Rev. B* 16, 1, 86
- [3]. De D K (2010) First observation of orthorhombic Jahn-Teller EPR spectra in Cu II doped $(\text{NH}_4)_2\text{Cd}_2(\text{SO}_4)_3 \cdot 6\text{H}_2\text{O}$ single crystals, Paper I, *African Physical review* 0011, 87
- [4]. Jona F and Pepinsky R (1956) In low energy electron diffraction (LEED) spectra. *Al. IBMJ. Res. Center, York Town*
- [5]. Kirste B (1992) Methods of automated analysis and simulation of EPR spectra. *Anal. Chim. Acta.* 191-200, 265
- [6]. Oguama F A (1997) EPR studies on the effect of magnetic Jahn-Teller and Jahn-Teller impurities on solid state phase transitions. *Doc. Dessert. Wake Forest Uni. USA.*
- [7]. Rabkin L. M, Torgashov V. I and Brezina B (1981) *Ferroelectrics* 36, 476
- [8]. Reynolds R. W and Boatner L. A (1975) Dynamic, intermediate and static Jahn-Teller in the EPR spectra of ^2E orbital states. *Phys. Rev B* 12, 4735
- [9]. Wu H (2006) EPR spectra simulation of anisotropic $1/2$ spin. Hanqing@csd.uwiii.edu.
- [10]. Yerima J. B (2005) EPR studies in the effect of paramagnetic impurities in phase transition and Jahn-Teller effect in crystalline solids: A review. *Tech and Dev Journal*, 9
- [11]. Yerima J. B (2007) EPR studies of the effect of paramagnetic impurity concentrations in phase transition and Jahn-Teller effect in crystalline solids. *Doc. Dissert. FUTY, Nigeria*
- [12]. Yerima J B and De D K (2014) Temperature Dependence of EPR Linewidth and Intensity in $\text{Cd}_2(\text{NH}_4)_2(\text{SO}_4)_3$ single crystals, *Vonuklang Multidisciplinary Journal of Science and Technology*, Vol 1, No.1